Dielectric relaxation studies of aqueous L-glutamine-ethanol mixtures in the microwave frequency range

T. Aiswarya [a], T. Vamshi Prasad [b], K.C. James Raju [a], T. Vishwam [c],*

[a] *School of Physics, University of Hyderabad, Hyderabad, Telangana 500046, India*
[b] *Department of Physics, Jawaharlal Nehru Technological University-Hyderabad, Hyderabad 500 085, India*
[c] *GITAM (Deemed to be University), Hyderabad Campus, Rudraram Village, Patancheru (M), Telangana 502329, India*

ABSTRACT

A study on the dielectric properties of various molar concentration levels of aqueous L-glutamine, ethanol mixtures at microwave frequency region ($0.02 < \nu/\text{GHz} < 20$) is carried out in the temperature range of 298 K to 323 K. Dielectric parameters such as dielectric permittivity, dielectric loss of different molar concentrations of L-glutamine in water, ethanol medium are evaluated. It is noticed that the real and imaginary part of dielectric permittivity increases with increase in molar concentration levels of L-glutamine in water and ethanol medium and decreases with increase in temperature. From these parameters, average relaxation time (τ), excessive inverse relaxation time $(1/\tau)^E$, excessive dielectric permittivity (ε^E) are determined and their behavior is analyzed in terms of the distribution of hydrogen bond network in the liquid medium. The theoretical dipole moments of L-glutamine in both aqueous and ethanol medium are determined by using DFT-B3LYP method with different solvation models. Mean molecular polarizability (α_M) of the system is calculated from the Lippincott δ function potential model and compared with the Lefevre method. The activation entropy (ΔS^*), activation enthalpy (ΔH^*), Helmholtz energy (ΔF^E) parameters have also been evaluated and the results are correlated.

© 2019 Elsevier B.V. All rights reserved.

1. Introduction

The aim of the Dielectric Relaxation Spectroscopy (DRS) is to investigate molecular interactions between the components present in the liquid system and also the variation in structural parameters due to hydrogen bonding [1–4]. The changes in the dielectric parameters provide information regarding the molecular dynamics in the liquid system. DRS technique is highly sensitive to detect structural changes in the molecule, intermolecular hydrogen bonding and orientation of the dipoles in liquid systems. Most of the biological systems contain the hydrogen bonds between molecules. This hydrogen bond plays a significant role in various biofunctional activities, metabolic reactions, protein synthesis, drug designing and electrical properties of the material [5,6]. The dielectric relaxation study of proteins in water as well as in alcoholic medium has received considerable attention due to bound water, zwitterionic nature and distribution of hydrogen bond network in the liquids. The understanding of intermolecular hydrogen bonding and typical relaxation behavior of protein solutions attracted many researchers for the study of interest in recent and past [7–20].

The dielectric relaxation behavior of protein in an aqueous medium is analyzed in terms of a superposition of three Debye relaxation processes in the microwave frequency region [21,22]. The first relaxation time at low frequency (τ_1) is due to rotational diffusion of the zwitterionic amino acid molecule. The second (τ_2) and third relaxation time (τ_3) are referred to co-operative dynamics of bulk water and fast localized motion of 'free water' molecules. The thermodynamic properties of aqueous glycine are determined as a function of pressure, temperature, and molality of the solution [23]. Qiushuo Yu et.al [24] studied the solubilities of L-glutamine in mixed solvents such as water + ethanol, water + acetone as a function of temperature and calculated dissolution enthalpy and entropy of L-glutamine in a water medium. The electromagnetic characteristic of basic amino acids in solution and its applications in microwave sterilization, as well as mechanism process, is explained by Chen Meng et al. [25]. Stelios Floros et al. [26] studied the dielectric function of lysozyme with molecular dynamics simulations and the results were interpreted in terms of hydration shell decomposition approach. Degtyarenko et al. [27] applied the Born-Oppenheimer molecular dynamics simulations of an aqueous L-alanine by considering the complete system relatively larger in size and has been treated fully quantum mechanically. Woese et al. [28] studied the interaction of amino acids with heterocyclic bases in pyridine solvents and also for the origin of the genetic code [29].

In the present manuscript, we report the molecular interaction behavior of L-glutamine in aqueous medium, aqueous L-glutamine in ethanol medium (R5-R20) [24] at various molar concentration levels by

---

* Corresponding author.
  E-mail address: vishwam.talloju@gitam.edu (T. Vishwam).

evaluating complex dielectric permittivity ($\varepsilon^* = \varepsilon' - j\varepsilon''$) in the frequency range $0.02 < \nu/\text{GHz} < 20$ between the temperatures 298 K–323 K. The average relaxation times of the systems are calculated from the Debye and Cole-Cole relaxation plots. By using Eyring's rate equation [30] thermodynamical parameters such as enthalpy of activation ΔH^*, the entropy of activation ΔS^* is determined. The strength of the interaction between L-glutamine in aqueous as well as an alcoholic solvent medium is interpreted in terms of single point energy calculations. These calculations are obtained by using DFT-B3LYP methods with Polarizable continuum model (PCM), Integral equation formalism (IEF-PCM) solvation models [31–33]. The mean molecular polarizability (α_M) [34,35] of L-glutamine in gaseous as well as water and ethanol medium is calculated from Lippincott δ function potential model and compared with the Lefevre method of polarizability values [36].

2. Experimental section

2.1. Chemicals

The chemicals used in this work such as L-glutamine, ethanol of analytical grade (purity 99%) were procured from SRL Pvt. Ltd., India. By using the standard distillation procedure, liquid samples are further purified under reduced pressure and collected only middle fractions. The collected mid fractions of the sample are saved in a dark bottle. The 4 Å molecular sieves are used to prevent moisture content in the sample. The purities of the liquids such as water and ethanol are verified by comparing the densities, ρ, refractive indices, n_D, dielectric permittivity (ε_0) measured at 20 MHz, dipole moment (μ) at 298 K with the available literature values and which are listed in Table 1 respectively. The measured parameter values are in good agreement with the reported values within the error limits.

2.2. Procedure followed for the dielectric measurements and parameters

One of the α-amino acids, L-glutamine is taken at different molar concentrations (0.05 M–0.25 M) with respect to the maximum solubility of L-glutamine in double distilled water. Further, this solution is prepared at different ratio with respect to the ethanol medium i.e., $R = 5, 10, 15, 20$ ($R = N_{\text{water}}/N_i$, N_i = molar ratio of ethanol) [24]. The complex dielectric permittivity of aqueous L-glutamine (GW) and aqueous L-glutamine-ethanol (GWE) mixtures were measured in the frequency range ($0.02 < \nu/\text{GHz} < 20$) with an open-ended coaxial probe kit (Keysight 85070 E) and a Vector Network Analyzer (Keysight E 8361C).The data is analyzed in terms of the lumped coaxial probe model [37,38]. The sample material is terminated with the open end of the coaxial line, reflection coefficient and impedance data are noted from the VNA. The permittivity of the sample is determined from the recorded data at that frequency and temperature. In order to vary the sample temperature, temperature controlled water bath system is used with an accuracy of ±0.01 K. Instead of measuring the dielectric permittivity of the sample directly, we measured the dielectric permittivity of some pure liquid samples such as water, acetone, ethanol and the data are recorded for the calibration purpose. The optical refractive index (n_D) of the liquid sample is measured by using the Abbe's refractometer in the temperature range 298 K–323 K with a variation of ±

0.01 K. The high frequency dielectric permittivity ($\varepsilon_\infty = n_D^2$) is determined from the measured refractive index data. The percentage of errors in the low frequency dielectric permittivity (ϵ_o) and optical refractive indexes (n_D) is 2% and 1% respectively. The percentage of error involved in the complex dielectric permittivity is ±2–3% respectively. The dielectric relaxation time (τ) of various concentrations of GW, GWE samples at different temperatures are calculated using Havriliak-Negami relation [39]. The Havriliak-Negami relation is used to fit the Debye and Cole-Cole [40,41] relaxation plots by using WINFIT software provided by Novocontrol Technologies. The experimental details and error analysis of open-ended coaxial probe technique and determination of excess dielectric parameters such as excess inverse relaxation time $(1/\tau)^E$, excess permittivity (ε^E) were reported in our previously published manuscript [42–44]. The dielectric relaxation time (τ) depends on this height of the potential barrier, a temperature dependent constant, and the average time required by an excited molecule to rotate from one equilibrium position to the other. Postulating on the analogy between the process of the dipole rotation and uni-molecular chemical reactions, Eyring [30] identified relation with Gibbs free energy of activation ΔG^*. His theory leads to an expression for τ as

$$\tau = \frac{h}{kT} \exp\left(\frac{\Delta G^*}{RT}\right) \tag{1}$$

i.e.,

$$\Delta G_* = 2.303 RT \, \log\left(\frac{\tau kT}{h}\right) \tag{2}$$

With, $\Delta G^* = \Delta H^* - T\Delta S_*$, one can write from Eq. (1)

$$\begin{aligned} \ln(\tau T) &= \ln\left(\frac{h}{k}\right) + (\Delta H^* - T\Delta S_*)/RT \\ &= \left[\ln\left(\frac{h}{k}\right) - \left(\frac{\Delta S_*}{R}\right)\right] + \left[\frac{\Delta H^*}{RT}\right] \end{aligned} \tag{3}$$

Thus, the slope of the linear plot between $\ln(\tau T)$ and $(1/T)$ gives $(\Delta H^*)/2.303R$, With the obtained value of ΔH^* and ΔS^*, ΔG^* can be calculated with the following relation

$$\Delta G^* = \Delta H^* - T\Delta S_* \tag{4}$$

where h is the Planck's constant, k is the Boltzmann constant and T is the temperature in Kelvin and R is the universal gas constant.

The mean molecular polarizability (α_M) of the L-glutamine in a different solvent medium is determined by considering the optimized bond lengths from the minimum energy-based conformer structure which is computed from DFT-B3LYP methods.

2.3. Computation details

The minimum energy-based geometry optimization procedure is followed for the single monomers of L-glutamine, ethanol and their binary system at gaseous state by using Hartree-Fock [45–47] and DFT-B3LYP methods [48–54] with 6-311G+ basis set. The density functional theory (DFT) offers a completely different approach to the calculation of

Table 1
The experimental data for the liquid samples used with the literature values at 298 K.

Liquid sample	Density ρ (g/cm³)		ϵ_0 (20 MHz)		n_D		Dipole moment (μ, D)		Relaxation time (τ, ps)	
	This work	Literature[a]	This work	Literature	This work	Literature[a]	This work	Literature	This work	Literature
Water	1.000	0.9970	78.51	78.54[a]	1.329	1.3330	1.85	1.85	8.47	8.39 [57]
Ethanol	0.788	0.7893	24.16	24.32 [58]	1.360	1.3614	1.68	1.69[a]	158.07	163 [58]

Standard uncertainties u are u(ρ) = 0.002, u(ε_0) = 2–3%, u(n_D) = 0.001, u(μ) = 0.02D and u(τ) = 5–7%.
[a] CRC handbook of chemistry and physics (2003–2004), 84th edition, Pg No:6-157,6-162, CRC Press.

molecular potentials. In contrast to the perturbation methods, this theory is not based on the refinement of a result obtained via Hartree–Fock but takes a different route to calculate the molecular energies [50,51]. The DFT methods derive these from a charge density $\rho(r)$, which depends only on the coordinates x, y, and z. The complete analysis of DFT methods started with Hohenberg and Kohn equation [52]. As per the first Hohenberg and Kohn theorem, instead of using a Slater determinant of spin-orbitals, by virtue of this theorem it is possible to calculate the total energy via the minimization of the charge density functional $E_{el}[\rho_{el}]$ which depends on the electron density

$$\rho_{(el)}(r) = \sum_i \left| \psi_i(r)^2 \right| \tag{5}$$

This is stated in the second Hohenberg–Kohn theorem, which proves that the energy obtained from a trial density ρ represents an upper bound to the true ground state energy, as obtained from the exact ground state density ρ_0. The energy in the DFT approach is not given as the expectation value of an operator, like in the HF approach but as a sum of energy functionals depending on the electron density:

The energy in the DFT approach is given by

$$E_{DFT}[\rho] = T(\rho) + V(\rho) + U(\rho) + E_{XC}(\rho) \tag{6}$$

where $T(\rho)$ describes the kinetic energy of the electrons, $V(\rho)$ the interaction with the nuclei, $U(\rho)$ the Coulomb repulsion between the electrons and $E_{XC}(\rho)$ the effects generated by the electron correlation which have no classical counterpart. This so-called exchange-correlation energy and it is used to collect all parts of the energy which cannot be handled exactly. According to the second Hohenberg–Kohn theorem, the total energy given by Eq. (6) obeys the relation:

$$E_0 \le E_{DFT}[\rho] \tag{7}$$

where E_0 is the true ground state energy. The equality holds only if the density inserted into Eq. (6) is the exact ground state density.

The effective DFT potential defined by

$$V^{DFT} = \int \frac{\rho(r')}{|r-r'|} dr' + V_{XC}(r) \tag{8}$$

where the first term is equivalent to the Coulomb–term of the HF equations, while V_{XC} is the potential due to the non-classical exchange-correlation energy E_{XC}. If the exact form of the exchange-correlation energy E_{XC} were known, the solution of the Kohn–Sham equation would generate the correct energy eigenvalue of the total Hamiltonian of the Schrodinger equation. So, while the HF model started with the approximation that the total wavefunction can be described by a single Slater determinant, and therefore cannot result in an exact solution, the Kohn–Sham approach is in principle exact. Unfortunately, the correct form of E_{XC} is not known, so the art of DFT calculations is to find good functional forms for this energy. A commonly used pair of functionals is Becke's 1988 exchange functional (B88 or B) [53] and the Lee-Yang-Parr (LYP) [54] correlation functional, or the so-called Becke3LYP (B3LYP) hybrid functional, which combines the B88 and LYP functionals via three parameters with three additional functionals. The parameters in these functionals are determined by fitting the results of the calculations for small molecular test systems to well established experimental molecular data.

Further, L-glutamine in an aqueous medium (GW), ethanol medium (GE) and aqueous L-glutamine in ethanol medium (GWE) are computed by using different solvation models like PCM and IEFPCM with the same basis set. The system is iterated a number of times to attain a minimum energy structure. From that point, dipole moment values are noted and tabulated in Table 5 respectively. Based on the single point energy calculations strength of the hydrogen bond interaction is determined.

Table 2
Low frequency dielectric permittivity (ε_0) measured at 20 MHz, high frequency dielectric permittivity and average relaxation time of L-glutamine in water (GW) and L-Glutamine-water-ethanol (GWE) of R5 to R20 with respect to molar concentration and temperature.

Con. (mol/L)	T (K)	glu-Water			R5			R10			R15			R20		
		ε_0	ε_∞	τ (ps)	ε_0	ε_∞	τ (ps)	ε_0	ε_∞	τ (ps)	ε_0	ε_∞	τ (ps)	ε_0	ε_∞	τ (ps)
	298	79.102	1.779	9.19	78.78	1.776	11.44	77.9	1.790	11.25	76.56	1.806	11.07	75.38	1.827	10.9
	303	77.555	1.776	9.09	77.04	1.774	11.19	76.93	1.787	10.43	75.5	1.803	10.34	74.64	1.825	10.24
	308	76.33	1.771	9	76.15	1.771	11.13	75.53	1.784	9.76	74.64	1.800	9.71	73.9	1.822	9.7
	313	75.065	1.768	8.907	75.13	1.768	10.70	74.64	1.782	9.64	73.98	1.798	9.52	72.86	1.819	9.16
	318	73.718	1.763	8.816	74.69	1.766	10.48	73.9	1.779	9.43	73.27	1.795	9.19	71.92	1.817	8.67
0.05	323	72.594	1.760	8.726	73.67	1.763	10.11	72.89	1.776	8.92	70.59	1.792	8.79	71.12	1.814	8.31
	298	79.856	1.787	11.44	79.61	1.782	11.52	78.91	1.795	11.29	77.96	1.811	11.24	77.44	1.833	11.05
	303	78.724	1.784	11.19	78.28	1.779	11.23	77.92	1.792	11.05	77.63	1.809	10.99	77.36	1.830	10.53
	308	77.397	1.779	11.10	77.6	1.776	11.16	77.62	1.790	11.03	77.52	1.806	10.51	77.1	1.827	10.43
	313	75.91	1.771	10.70	76.18	1.774	10.93	77.98	1.787	10.45	76.92	1.803	10.12	76.8	1.825	10.1
	318	74.917	1.768	10.48	75.73	1.771	10.74	76.73	1.784	10.17	76.55	1.800	10.04	75.93	1.822	9.94
0.1	323	73.432	1.763	10.11	74.73	1.768	10.20	75.95	1.782	10.10	74	1.798	9.89	74.15	1.819	9.81
	298	80.279	1.806	12.48	80.96	1.787	12.48	80.93	1.803	12.27	79.28	1.817	11.80	78.85	1.827	11.59
	303	79.075	1.798	11.61	80.01	1.784	11.61	79.05	1.800	11.57	78.98	1.814	11.44	78.6	1.825	10.88
	308	77.78	1.792	11.29	79.24	1.782	11.29	78.91	1.798	11.09	78.65	1.800	11.00	78.24	1.822	10.78
	313	76.294	1.784	11.24	79	1.779	11.24	78	1.795	10.90	77.93	1.809	10.70	77.37	1.819	10.46
	318	75.296	1.779	10.80	78.45	1.776	10.80	77.82	1.792	10.69	76.91	1.806	10.30	76.67	1.817	10.14
0.15	323	73.892	1.774	10.28	77	1.774	10.28	76.96	1.790	10.19	75.07	1.803	10.07	75.41	1.814	19.81
0.2	298	80.400	1.825	13.10	81.2	1.792	13.10	80.93	1.809	12.68	80.13	1.822	12.46	79.97	1.838	12.26
	303	79.293	1.814	12.17	80.81	1.790	12.27	79.94	1.806	11.78	79.63	1.819	11.59	79.5	1.836	11.46
	308	77.827	1.811	11.42	80.45	1.787	11.51	79.66	1.803	11.30	79.54	1.817	11.43	78.3	1.833	11.33
	313	76.75	1.809	11.28	79.82	1.784	11.31	78.82	1.800	11.16	78.7	1.814	11.09	77.57	1.830	10.62
	318	75.280	1.798	10.31	78.97	1.782	10.98	78.13	1.798	10.94	77.98	1.811	10.71	76.87	1.827	10.51
	323	74.057	1.792	10.12	77.73	1.779	10.43	77.29	1.795	10.34	75.85	1.809	10.31	75.64	1.825	9.78
0.25	298	80.514	1.838	13.81	82.2	1.800	13.50	81.92	1.814	12.89	81.52	1.827	12.65	81	1.844	12.65
	303	79.369	1.836	12.50	81.2	1.798	12.50	80.82	1.811	12.27	80.24	1.825	12.16	80.07	1.841	11.74
	308	78.264	1.825	11.70	80.9	1.795	11.70	79.87	1.809	11.58	79.2	1.822	15.52	79.01	1.838	11.42
	313	76.87	1.822	10.76	80.1	1.792	11.50	78.91	1.806	11.32	78.16	1.819	11.25	78	1.836	11.06
	318	75.824	1.817	10.87	79.2	1.790	11.20	78.11	1.803	10.95	77.75	1.817	10.90	77.34	1.833	10.62
	323	74.988	1.814	10.28	78.3	1.787	10.76	77.5	1.800	10.47	77	1.814	10.75	76.99	1.830	10.04

Standard uncertainties u are $u(\varepsilon_0)$ = 2–3%, $u(\varepsilon_\infty)$ = 0.001, and $u(\tau)$ = 5–7%.
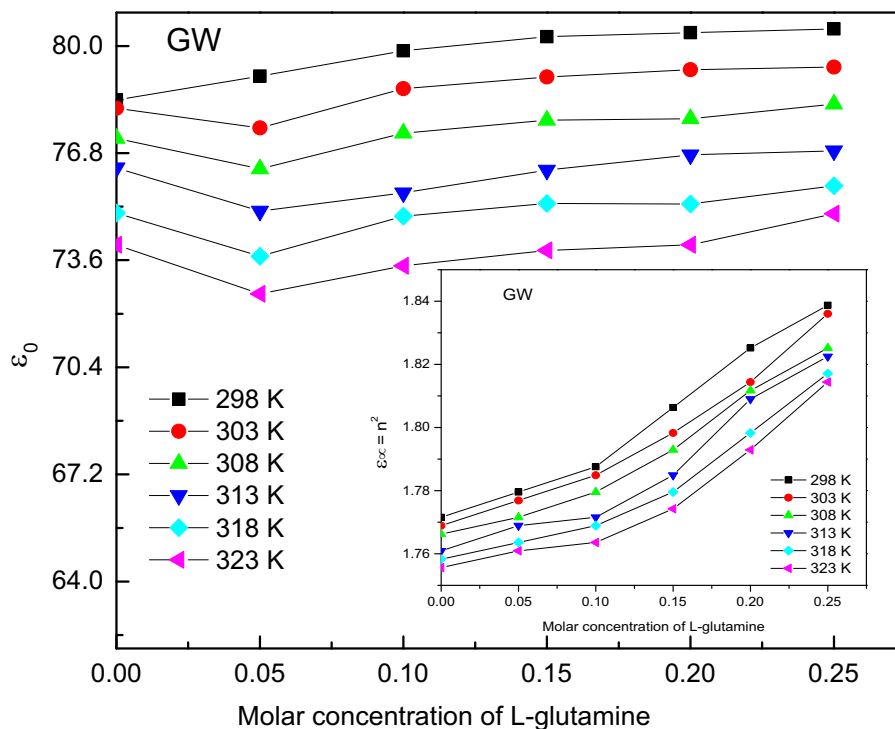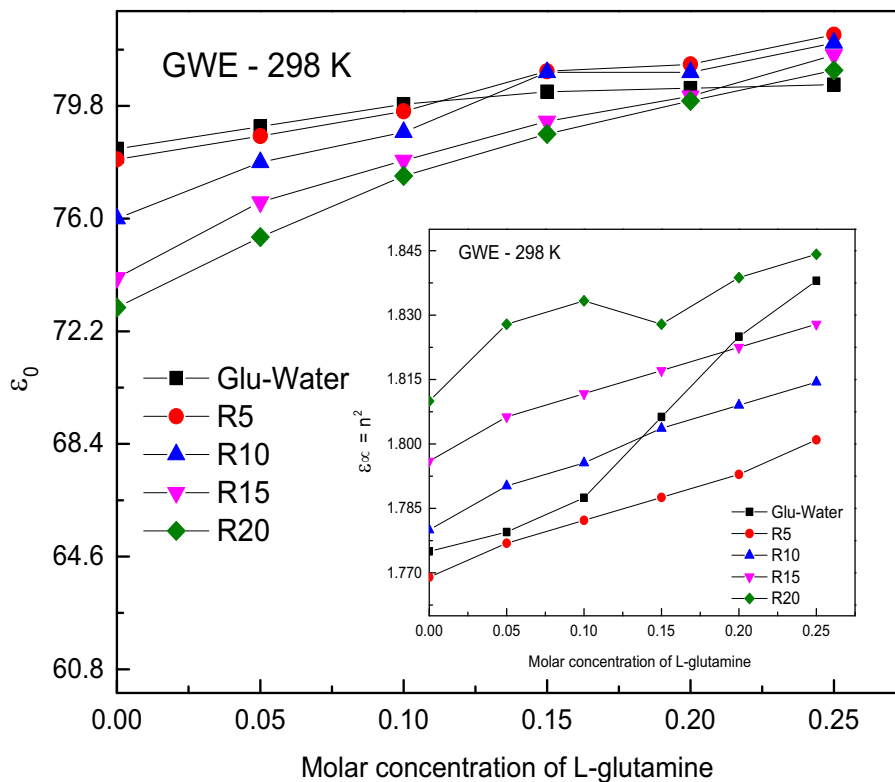
Fig. 1. Low frequency dielectric permittivity (ϵ_0) measured at 20 MHz and high frequency dielectric permittivity ($\epsilon_\infty = n^2$) versus molar concentration of L-glutamine in water (GW) at different temperatures.

3. Results and discussion

The low frequency dielectric permittivity (ϵ_o) of various molar concentration levels of aqueous L-glutamine (GW) and aqueous L-glutamine in ethanol (GWE) medium are measured at 20 MHz at different temperatures are tabulated Table 2 respectively. It is observed that low frequency dielectric permittivity (ϵ_o) value is increased with increase in the Glutamine concentration in water and

Fig. 2. Low frequency dielectric permittivity (ϵ_0) measured at 20 MHz and high frequency dielectric permittivity ($\epsilon_\infty = n^2$) versus molar concentration of aqueous L-glutamine in ethanol (GWE) at 298 K.
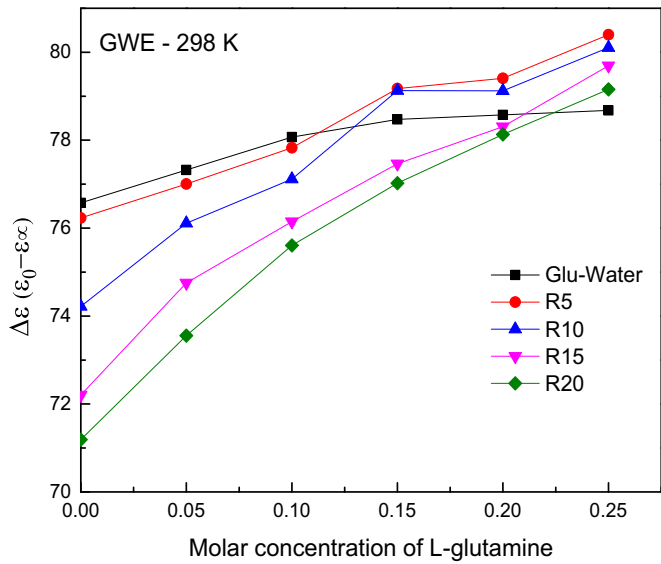
Fig. 3. The dielectric relaxation strength (Δε) versus molar concentration of ʟ-glutamine at 298 K.

it may be due to bound water phenomena (see Fig. 1) [22,55,56]. The magnitude of the low frequency dielectric permittivity (ϵ_o) value of aqueous ʟ-glutamine (GW) is greater when compared to the aqueous

ʟ-glutamine in ethanol (GWE) for all concentration levels of R5 to R20, and these values decrease with increase in temperature (Table 2). Whereas within the R5-R20 concentrations, the dielectric permittivity value increased with increase in the ʟ-glutamine concentration and it may be due to the formation of hydrogen bonds between Glutamine-water-ethanol systems which is as shown in Fig. 2 at 298 K. The newly formed hydrogen bonds try to modify the structure of the liquid system and enhance the dielectric permittivity values. A similar trend is observed for the remaining temperatures (Table 2).

Further, the increase in the aqueous concentration in ethanol medium i.e. R5-R20, the dielectric permittivity value decreases and it is due to a decrease in the electrical susceptibility of the medium. The decrease in the electrical susceptibility may be due to the presence of multimers in the binary solution. The formed multimers are oriented randomly and cause depolarization effect in the liquid medium. The decrease in low frequency dielectric permittivity (ϵ_o) values of GW and GWE with an increase in temperature due to a decrease in the degree of orientation of the dipoles. The rise in temperature disturbs the alignment of the dipoles in the field direction and it leads to a decrease in the dielectric permittivity values.

From high frequency dielectric permittivity values ($\epsilon_\infty = n_D^2$), there is an increase in the refractive index values with increase in molar concentration of ʟ-glutamine in water (GW) as well GWE (R5-R20) medium due to the formation of hydrogen bond network in the system. The variation of low frequency and high frequency dielectric permittivity with mole fraction at all temperatures shows non-linear behavior
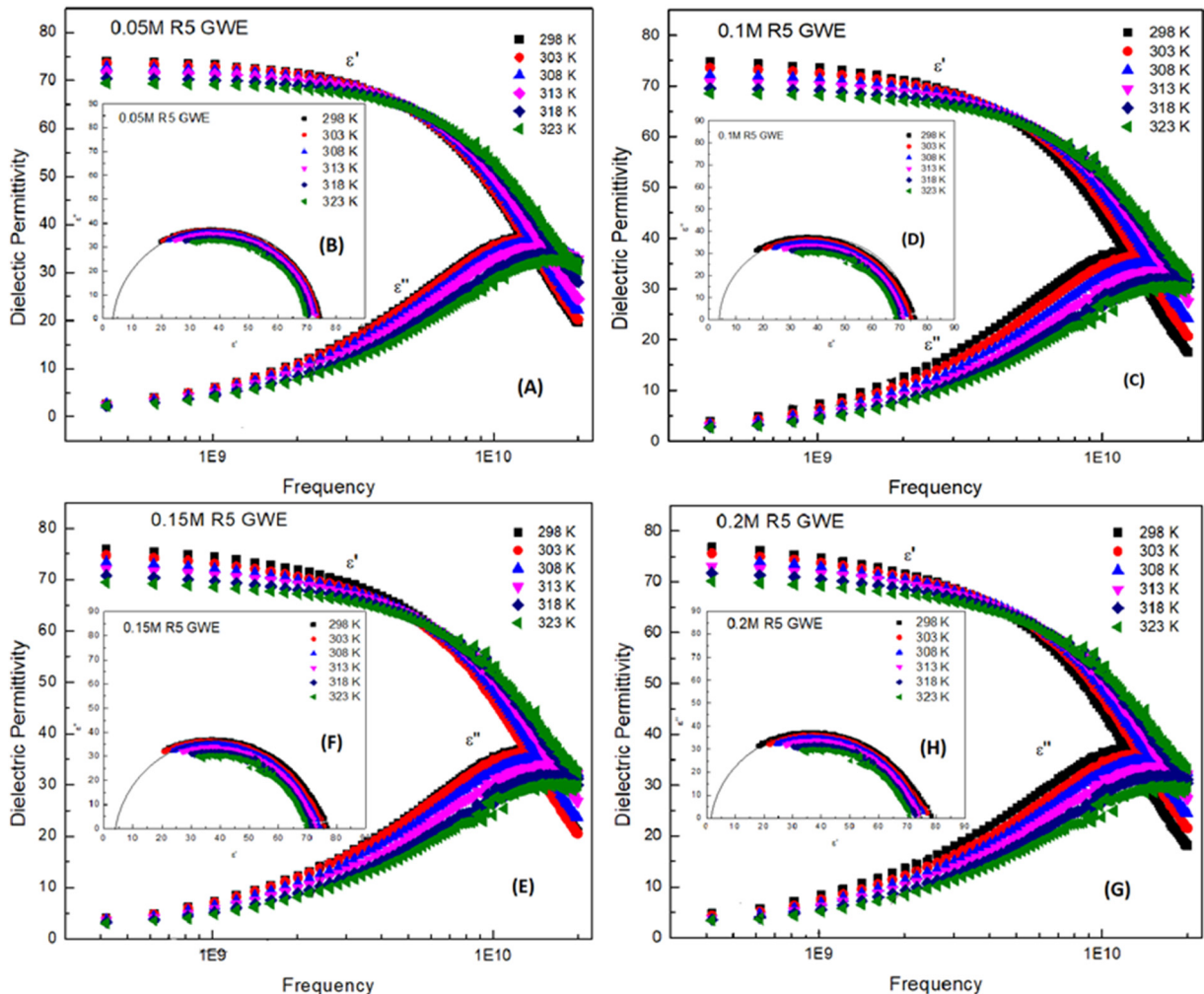

Fig. 4. A), C), E) and G) Frequency-dependent of dielectric permittivity (ε′-j ε″) and complex plane plot (B, D, F, H) of ε″ vs ε′ of R5 (0.05 M–0.2 M) at different temperatures.
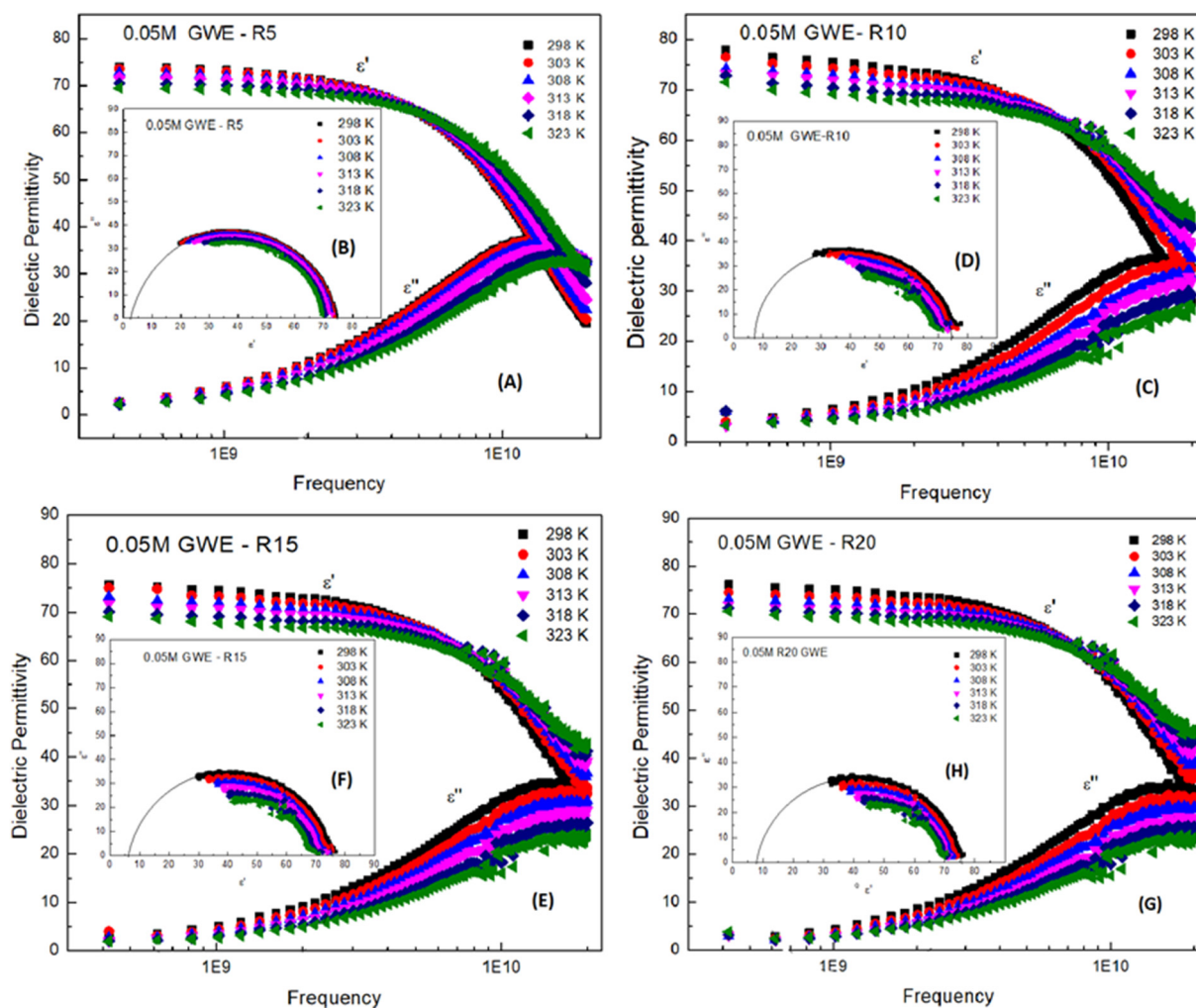
Fig. 5. A), C), E) and G) Frequency-dependent of dielectric permittivity (ε'-j ε") and complex plane (B, D, F, H) plot of ε" vs ε' of 0.05 M concentration of GWE (R5–R20) at different temperatures.

(Figs. 1 and 2). This non-linear behavior indicates the presence of hetero-molecular interaction that takes place in the aqueous L-glutamine (GW) and aqueous L-glutamine-ethanol (GWE) system. The dielectric relaxation strength parameter, i.e., $\Delta\epsilon = (\epsilon_o$-$\epsilon_\infty)$ indicates the presence of clusters in the solution. These clusters are formed in the solution due to the cooperative process of multimers (aggregation of a greater number of polar groups) with hydrogen bonded linkage. From Fig. 3, it is noted that the dielectric field strength value increased with increase in the glutamine concentration in water (GW) as well as ethanol (GWE) medium which indicates the presence of clusters the solution. The dielectric relaxation strength value decreases with increase in temperature and it is due to the breakage of hydrogen bonds between the multimers restricting the free movement of polar molecules in the liquid medium.

The real and imaginary part of the dielectric permittivity (ε^*=ε'-jε") of R5 of different molar concentration (0.05 M–0.2 M) of GWE, and also for fixed 0.05 M concentration of R5 to R20 at different temperature are shown in Figs. 4 and 5 respectively. It is marked that the real part of dielectric permittivity decreases with increase in frequency and the temperature. Further, from Fig. 4(A to G), it is noticed that the dielectric loss peak shifts towards higher frequencies with an increase in the concentration of L-glutamine in the water-ethanol system (GWE) and it is due to the formation of hydrogen bonds between Glutamine and water-ethanol system. Due to the increase in the chain length of the system, it takes more energy to oscillate from one mean position to another mean position. Whereas in the Fig. 5(A–G) for 0.05 M concentration, the

dielectric loss is slightly higher for R5 of GWE when compared to R10–R20 and decreases with increase in temperature. From Figs. 4 and 5, it is also noticed that there is broadening of the dielectric loss peak
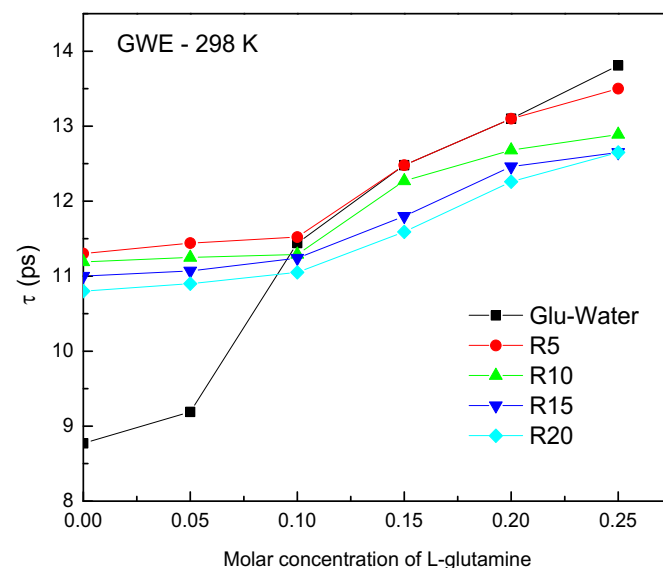

Fig. 6. The relaxation time (τ/ps) versus molar concentration of L-glutamine at 298 K.
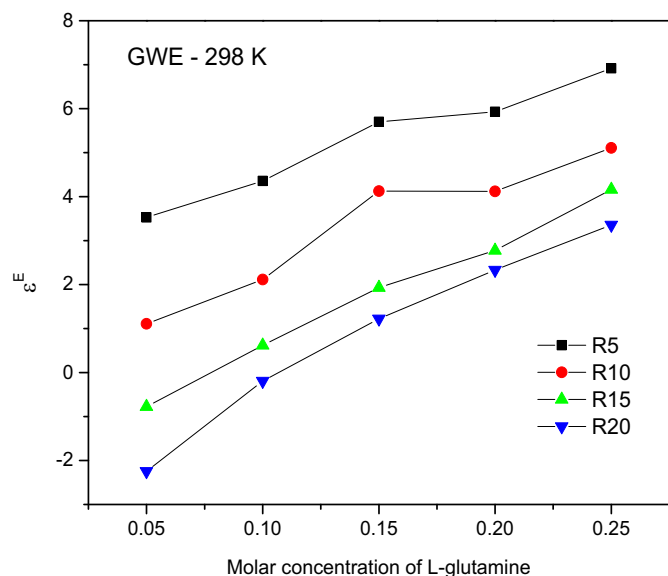
Fig. 7. The excessive dielectric permittivity (ε^E) versus molar concentration of L-glutamine at 298 K.

all the measured temperature range i.e., 298 K–323 K. From Table 2, it is noticed that higher values of the relaxation times observed for mixtures of higher concentration of L-glutamine in water and as well as ethanol system for all levels of R5 to R20. It is due to the reorientation of aqueous L-glutamine in ethanol molecules occurs slower than that of water molecules. Since water molecules bound to L-glutamine molecules possess higher relaxation time values than the relaxation time of free water molecules. The increase in the molar concentration of L-glutamine in GW and GWE, relaxation time continues to increase which is as shown in Fig. 6 at 298 K. The aqueous L-glutamine in ethanol medium cooperates in the formation of an increase in the hydrogen bonds that enhance the relaxation time. Similar behavior is observed for remaining concentrations. There is a decrease in the relaxation time values with an increase in temperature due to the disturbance in the alignment of the dipoles. The excess dielectric permittivity (ε^E) indicates the presence of molecular interaction taking place in the liquid mixture in terms of hydrogen bonding. If the excess dielectric permittivity values are positive, it indicates the higher macroscopic permittivity values and it may be due to the presence of a greater number of dipoles in the solution due to hydrogen bonding when compared to the pure system. From Fig. 7, it is observed that ε^E values are positive which indicates the average number of dipoles formed in the mixture is greater than the individual system. From Fig. 8, it is noticed that for all the molar concentrations of aqueous L-glutamine in ethanol i.e. R5 to R20, the excess inverse relaxation time $(1/\tau)^E$ shows a negative trend for all temperatures. This indicates the effective dipoles rotate slowly in the mixture due to the presence of hydrogen bond between aqueous L-glutamine with ethanol medium. The increase in the chain length and also the existence of multimers in the solution is further responsible for the slower rotation of the dipoles in the liquid mixtures.

The enthalpy of activation ΔH^* for the dielectric relaxation process of GW is smaller when compared to the GWE (R5-R20) concentrations which are tabulated in Tables 3 and 4. The enthalpy of activation ΔH^*

(dispersion) with an increase in the concentration of Glutamine and the temperature and it may be due to the fluctuations of hydrogen bond network in the GWE system.

The average relaxation times of the GW and GWE system are calculated from the complex plane plot of ε'' vs ε' i.e., Debye and Cole-Cole plots and are as shown in Figs. 4 and 5 (inserted fig) and are tabulated in Table 2 respectively. In a Cole-Cole relaxation plot the value of α is in the range of $0.912 < \alpha < 1$ for all the concentrations of GW, GWE at
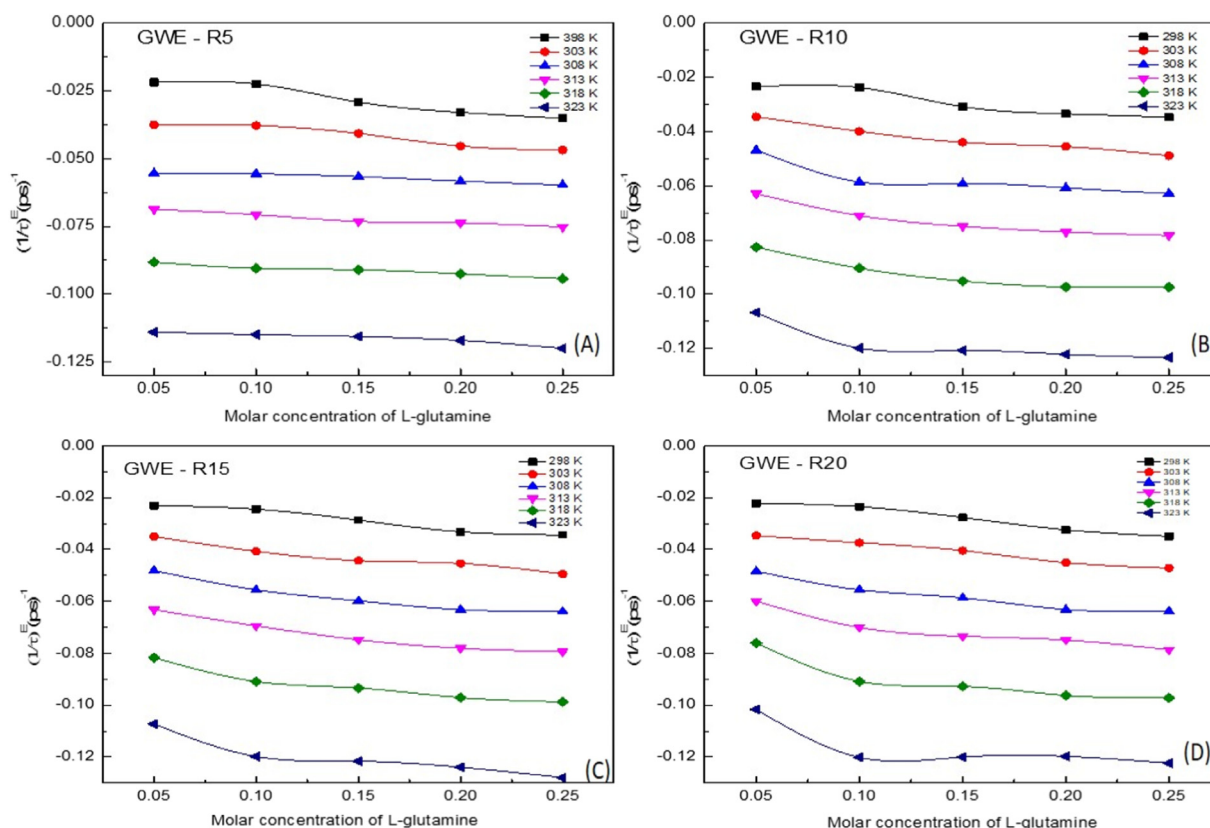

Fig. 8. A), B), C) and D) experimental values of excessive relaxation time $((1/\tau)^E)$ versus molar concentration of L-glutamine at different temperatures.

Table 3
Variation of thermodynamical parameters ΔG^*, ΔH^* and ΔS^* with respect to the molar concentration of L-glutamine in water (GW) and in ethanol (GWE) of R5 to R10 combinations with temperature.

Con mol/L	T (K)	glu-Water ΔH*/(kcal/mol)	ΔG*/(kcal/mol)	ΔS*/(Cal/mol/K)	R5 ΔH*/(kcal/mol)	ΔG*/(kcal/mol)	ΔS*/(Cal/mol/K)	R10 ΔH*/(kcal/mol)	ΔG*/(kcal/mol)	ΔS*/(Cal/mol/K)
	298		10.021	96.14		10.565	−25.17		10.522	−3.10
	303		10.203	94.50		10.728	−25.30		10.550	−3.15
	308		10.388	93.23		10.933	−25.55		10.596	−3.24
	313		10.572	91.97		11.049	−25.52		10.779	−3.78
	318		10.755	90.73		11.213	−25.63		10.934	−4.20
0.05	323	1953	10.939	89.24	3.062	11.334	−25.61	9.597	11.001	−4.34
	298		10.564	−3.10		10.580	−25.55		10.530	−24.89
	303		10.727	−3.15		10.736	−25.64		10.696	−25.03
	308		10.932	−3.24		10.939	−25.89		10.910	−25.31
	313		11.049	−3.78		11.104	−26.00		10.987	−25.16
	318		11.213	−4.20		11.277	−26.14		11.134	−25.22
0.1	323	3006	11.334	−4.34	2.966	11.359	−25.99	3.113	11.331	−25.44
	298		10.779	−24.89		10.780	−13.84		10.737	−14.09
	303		10.863	−25.03		10.820	−13.74		10.811	−14.10
	308		10.969	−25.31		10.969	−14.00		10.924	−14.24
	313		11.177	−25.16		11.178	−14.45		11.098	−14.57
	318		11.292	−25.22		11.292	−14.58		11.265	−14.86
0.15	323	7141	11.379	−25.44	6.656	11.378	−14.62	6.539	11.356	−14.91
	298		10.899	−14.09		10.890	−4.30		10.819	−11.72
	303		10.939	−14.10		10.959	−4.45		10.857	−11.65
	308		10.998	−14.24		11.018	−4.57		10.972	−11.83
	313		11.187	−14.57		11.203	−5.09		11.159	−12.24
	318		11.169	−14.86		11.336	−5.43		11.327	−12.58
0.2	323	13,039	11.337	−14.91	9.610	11.419	−5.60	7.328	11.394	−12.59
	298		11.030	−11.72		10.974	−4.17		10.859	−6.72
	303		11.006	−11.65		11.006	−4.20		10.960	−6.94
	308		11.060	−11.83		11.060	−4.31		11.034	−7.07
	313		11.064	−12.24		11.237	−4.81		11.197	−7.48
	318		11.309	−12.58		11.388	−5.21		11.328	−7.77
0.25	323	23,742	11.379	−12.59	9.732	11.502	−5.48	8.856	11.429	−7.96

Table 4
Variation of thermodynamical parameters ΔG^*, ΔH^* and ΔS^* with respect to the molar concentration of L-glutamine in water (GW) and in ethanol (GWE) of R15 and R20 combinations with temperature.

Con (mol/L)	T (K)	R15 ΔH*/(kcal/mol)	ΔG*/(kcal/mol)	ΔS*/(Cal/mol/K)	R20 ΔH*/(kcal/mol)	ΔG*/(kcal/mol)	ΔS*/(Cal/mol/K)
0.05	298	9.950	10.483	−1.79	12.278	10.444	6.15
	303		10.527	−1.91		10.503	5.86
	308		10.584	−2.06		10.582	5.51
	313		10.745	−2.54		10.646	5.22
	318		10.868	−2.89		10.712	4.92
	323		10.961	−3.13		10.909	4.24
0.1	298	8.430	10.519	−7.01	2.666	10.479	−26.22
	303		10.682	−7.43		10.573	−26.10
	308		10.786	−7.65		10.767	−26.30
	313		10.904	−7.91		10.854	−26.16
	318		11.100	−8.40		11.074	−26.44
	323		5.092	10.33		11.256	−26.59
0.15	298	5.973	10.640	−15.66	5.404	10.597	−17.42
	303		10.782	−15.87		10.655	−17.33
	308		10.901	−16.00		10.851	−17.69
	313		11.049	−16.22		10.989	−17.84
	318		11.167	−16.33		11.126	−17.99
	323		11.324	−16.57		11.253	−18.11
0.2	298	6.835	10.775	−13.22	8.431	10.742	−7.75
	303		10.838	−13.21		10.783	−7.76
	308		11.000	−13.52		10.978	−8.27
	313		11.143	−13.76		11.030	−8.30
	318		11.269	−13.94		11.220	−8.77
	323		11.387	−14.09		11.299	−8.88
0.25	298	6.395	10.813	−14.82	9.769	10.813	−3.50
	303		10.937	−14.99		10.849	−3.57
	308		11.020	−15.02		10.997	−3.99
	313		11.181	−15.29		11.135	−4.37
	318		11.317	−15.48		11.248	−4.65
	323		11.498	−15.80		11.315	−4.79

depends upon the entities present in the surrounding medium. The difference in the enthalpy of activation energies between GW and GWE shows positive values which indicates the presence of multimers in the solutions that may form the bonds and break the bonds at different extents. The entropy is a measure of disorder in the system. If the surrounding entity or local environment of the system is supportive of the activated process, then the system becomes more stable in nature when compared to the normal system. The change in entropy for the normal system is negative. If the entropy of the system is positive that indicates a non-cooperative environment in the system and the activated system is in unstable condition. In the present study, the entropy of activation ΔS^* value is found to be negative for all the cases such as GW and GWE (R5-R20) except GW for 0.05 molar concentration and it may be due to the presence of a smaller number of hydrogen bonds (less concentration of Glutamine). There is a change in the magnitude of the ΔS^* indicates the fluctuations in the formation of a hydrogen bond network in the liquid system.

The experimental dipole moment values are compared with the theoretical dipole moment values which are calculated from the DFT-B3LYP method with 6-311G+ basis sets are tabulated in Table 5. In order to determine the theoretical dipole moment values of the individual and binary system, we have used different solvation models such as IEFPCM and PCM. From the theoretically computed dipole moment values (Table 5) it is observed that there is a slight increase in the effective dipole moment values of GWE when compared to the individual water (GW) and ethanol system (GE). Whereas dipole moment value of L-glutamine in a gaseous state is higher when compared to the GWE, GE and GW systems. The decrease in the effective dipole moment values when compared to the gaseous state may be due to the hydrogen-bonded network and distribution of charges in the system. The single point minimum energy is also calculated for an individual and binary system. The difference in energy level between GWE-GW, GWE-GE system is around 11–16 kcal/mol, which indicates there exists a strong hydrogen bond between the components present in the system.

The mean molecular polarizability (α_M) of the L-glutamine in a gaseous state, aqueous, ethanol as well as ethanol-water medium is calculated by using Lippincott δ function potential model and verified with Lefevre method of polarization which is tabulated in Table 5. The values are in close agreement with each other. In order to determine the polarizability values, we have considered the optimized bond length values from the minimum energy based confirmed structure obtained from DFT calculations. There is a small difference in the polarizability values of GWE when compared to the GW, GE, and L-glutamine (gas medium) which indicates that the presence of hydrogen bond between the glutamine-water-ethanol system.

4. Conclusions

The study of complex dielectric permittivity ($\varepsilon^* = \varepsilon' - j\varepsilon''$) of L-glutamine in Water (GW), aqueous L Glutamine in ethanol (GWE) mixtures at various molar concentration levels are summarized in the frequency region of $0.02 < \nu/GHz < 20$ at different temperatures. The following results are outlined from the study;

- The dielectric permittivity (ε_0), relaxation time (τ) and field strength ($\Delta\varepsilon$) increased with increase in L-glutamine concentration in water as well as ethanol system and it is due to the presence of multimers in the solution through hydrogen bonding and its values decrease with increase in temperature.
- The values of Gibbs free energy activation (ΔG^*) are positive which shows the presence of multimers in the solution due to hydrogen bond interaction.
- The variation of entropy of activation ΔS^* values indicates that the fluctuations in the formation of the hydrogen bond network in the liquid system are due to temperature and environment in the liquid system.

Table 5
Theoretical dipole moment and mean molecular polarizability of L-glutamine molecule in a gaseous state, aqueous (GW), ethanol (GE) and water-ethanol (GWE) solvent medium is calculated from the different quantum mechanical methods.

State	Gaseous state			In water medium (GW)				In ethanol medium (GE)				In water + ethanol medium (GWE)	
Model	Hartree-Fock	DFT-B3LYP	Exptl. value from literature	IEFPCM Hartree-Fock	IEFPCM DFT-B3LYP	PCM Hartree-Fock	PCM DFT-B3LYP	IEFPCM Hartree-Fock	IEFPCM DFT-B3LYP	PCM Hartree-Fock	PCM DFT-B3LYP	IEFPCM DFT-B3LYP	PCM DFT-B3LYP
Basis set	6-311G*	6-311G*		6-311G*	6-311G*	6-311G*	6-311G*	6-311G*	6-311G*	6-311G*	6-311G*	6-311G*	6-311G*
Dipole moment (Debye)	4.374	4.393	15.1 [17]	2.976	2.972	2.920	2.148	2.791	2.790	2.790	2.791	2.997	2.994
Energy (a.u)	−531.93	−531.30	–	−528.86	−528.81	−528.80	−528.82	−531.94	−531.93	−531.91	−531.90	−531.95	−531.92
Polarizability ($\times 10^{-25}$ cm^{-3}) by Lippincott δ-function model	134.126	135.123	–	145.74	145.74	146.32	146.65	134.67	136.67	135.57	135.47	136.34	136.38
Polarizability ($\times 10^{-25}$ cm^{-3} cm^{-3}) by Lefevre method	134.75	134.75	–	134.75	134.75	134.75	134.75	134.75	134.75	134.75	134.75	134.75	134.75

- There is a change in the mean molecular polarizability values of the GWE when compared to GW and GE system which reveals the presence of the hydrogen bond between the liquid system.
- The energy difference between GWE-GW, GWE-GE system is around 11–16 kcal/mol, which confirms the existence of a strong hydrogen bond between the components present in the system.
- The mean molecular polarizability values obtained from Lippincott δ function potential model are well in agreement with the Lefevre method of polarizability values.
- These studies are further useful in understanding the protein interactions in different solvent medium to interpret hydrogen bond interactions and their relaxation behavior phenomena.

Acknowledgments

References

[1] R.J. Sengwa, Vinita Khatri, Sonu Sankhla, Fluid Phase Equilib. 266 (2008) 54–58.
[2] A.V. Patil, V.P. Pawar, J.Mol.Liq. 188 (2013) 1–4.
[3] P. Jeevanandham, S. Kumar, P. Periyasamy, A.C. Kumbharkhane, Adv. Phys. Chem. (2014) 2014–2022.
[4] H.A. Chaube, V.A. Rana, P. Hudge, A.C. Kumbharkhane, J. Mol. Liq. 211 (2015) 346–352.
[5] Guo-Zhu Jia, Qian Jie, Wang Feng, J. Mol. Struct. 1100 (2015) 354–358.
[6] S. Scheiner, Hydrogen Bonding, Oxford University Press, New York, 1997.
[7] Roger B. Grgory, Protein-Solvent Interactions, Marcel Dekker. Inc, U.S.A2 h, 1995.
[8] R. Pethig, Dielectric and Electronic Properties of Biological Materials, Wiley, Chichester, 1979.
[9] M.W. Aaron, E.H. Grant, Br. J. Appl. Phys. 18 (1967) 957–960.
[10] Masaharu Kumazaki, Shintaro Sugai, J. Phys. Soc. Jpn. 32 (1971) 785–791.
[11] U. Kaatze, P. Schmidt, R. Pottel, J.Mol.Liq. 52 (1992) 181–210.
[12] Nilashis Nandi, Biman Bagchi, J. Phys. Chem. B 101 (50) (1997) 10954–10961.
[13] Somedatta Pal, Sanjoy Bandyopadhyay, Langmuir, 29 (4) (2013) 1162–1173.
[14] Georgios Archontis, Thomas Simonson, J. Am. Chem. Soc. 123 (44) (2001) 11047–11056.
[15] K. Modig, E. Liepinsh, G. Otting, B. Halle, J. Am. Chem. Soc. 126 (1) (2004) 102–114.
[16] Stefan Boresch, Martin Willensdorfer, Othmar Steinhauser, J. Chem. Phys. 120 (2004) 3333–3347.
[17] Elena Pirogova, George P. Simon, Irena Cosic, IEEE Trans. Nanobioscience 2 (2) (2003) 63–69.
[18] Thorsten Hansen, Lasse Jensen, Per-Olof Åstrand, Kurt V. Mikkelsen, J. Chem. Theory Comput. 1 (4) (2005) 626–633.
[19] C. Cametti, S. Marchett, C.M.C. Gambi, G. Onori, J. Phys. Chem. B 115 (21) (2011) 7144–7153.
[20] Iñigo Rodríguez-Arteche, Silvina Cerveny, Ángel Alegríaa, Juan Colmenero, Phys. Chem. Chem. Phys. 14 (2012) 11352–11362.
[21] T. Sato, R. Buchner, A. Frenandez, A. Chiba, W. Kunz, J. Mol. Liq. 117 (2005) 93–98.
[22] M. Wolf, R. Gulich, P. Lunkenheimer, A. Loidl, Biochim. Biophys. Acta, Proteins Proteomics (2012) 1–11.
[23] Darren Rowland, J. Phys. Chem. Ref. Data 47 (2018), 023104.
[24] Qiushuo Yu, Xiaoxun Ma, Long Xu, Thermochim. Acta 558 (2013) 6–9.
[25] Chen Meng, Fan Da-ming, Huang Lue-lue, Gao Yi-shu, Huang Jian-lian, Zhao Jian-xin, Zhang Hao, Innov. Food Sci. Emerg. Technol. 41 (2017) 100–108.
[26] S. Floros, M. Liakopoulou-Kyriakides, K. Karatasos, G.E. Papadopoulos, Eur. Biophys. J. 44 (8) (2015) 599–611.
[27] Ivan M. Degtyarenko, Karl J. Jalkanen, Andrey A. Gurtovenko, Risto M. Nieminen, J. Phys. Chem. B 111 (2007) 4227–4234.
[28] C. Woese, D. Dugre, W. Saxinger, S. Dugre, Proc. Natl. Acad. Sci. 55 (1966) 966–974.
[29] C. Woese, Evolution of the genetic code, Naturwissenschaften 60 (1973) 447–459.
[30] H. Eyring, J.Chem.Phys. 4 (1926) 283–291.
[31] E. Canses, B. Mennucci, J. Tomasi, J. Chem. Phys. 107 (1997) 3032–3041.
[32] J. Tomasi, M. Persico, Chem. Rev. 94 (1994) 2027–2094.
[33] J. Tomasi, B. Mennucci, R. Camm, Chem. Rev. 105 (2005) 2999–3094.
[34] E.R. Lipincott, J.M. Stutman, J. Phys. Chem. 68 (1964) 2926–2940.
[35] A.A. Frost, B. Musulin, J. Chem. Phys. 22 (1954) 1017–1020.
[36] R.J.W. Le Fèvre, A.J. Williams, J. Chem. Soc. 0 (1965) 4185–4188.
[37] Y.Z. Wei, S. Sridhar, Rev. Sci. Instrum. 60 (1989) 3041–3046.
[38] U. Kaatze, Metrologia 47 (2010) S91–S113.
[39] S. Havriliak, S. Negami, Polymer 8 (1967) 161–210.
[40] K.S. Cole, R.H. Cole, J. Chem. Phys. 9 (1941) 341–352.
[41] N.E. Hill, W.E. Vaughen, A.H. Price, M. Davies, Dielectric Properties and Molecular Behavior, Van Nostard Reinhold, London, 1969.
[42] V. Manjula, T. Vamshi Prasad, K. Balakrishna, V.R.K. Murthy, T. Vishwam, Spectrochim. Acta A 222 (2019), 117274.
[43] T. Vishwam, Suriya Shihab, S. Sreehari Sastry, Ha SieTiong, V.R.K. Murthy, Spectrochim. Acta A 179 (2017) 74–82.
[44] T. Vishwam, K. Parvateesam, S. Sreehari Sastry, V.R.K. Murthy, Spectrochim. Acta A 114 (2013) 520–530.
[45] R. Hartree, Proc. Camb. Philos. Soc. 24 (1928) 89–110.
[46] V. Fock, Z. Phys. 61 (1930) 126–148.
[47] J.C. Slater, Phys. Rev. 35 (1930) 210–211.
[48] R.G. Parr, W. Yang, Density-Functional Theory of Atoms and Molecules, Oxford University Press, New York, 1994.
[49] A.D. Becke, J. Chem. Phys. 98 (1993) 1372–1377.
[50] W. Koch, M.C. Holthausen, A Chemist's Guide to Density Functional Theory, Second edition Wiley-VCH, Weinheim, 2001.
[51] W. Kohn, Rev. Mod. Phys. 71 (1999) 1253–1266.
[52] P. Hohenberg, W. Kohn, Phys. Rev. 136 (1964) B864.
[53] A.D. Becke, J. Chem. Phys. 98 (1993) 5648–5652.
[54] C. Lee, W. Yang, R.G. Parr, Phys. Rev. B 37 (1988) 785–789.
[55] R.B. Talware, P.G. Hudge, Y.S. Joshi, A.C. Kumbharkhane, Phys. Chem. Liq. 50 (2012) 102–112.
[56] Ajay Chaudhari, A.G. Shankarwar, B.R. Arbad, S.C. Mehrotra, J. Solut. Chem. 33 (2004) 313–322.
[57] Liana S. Gabrielyan, J. Mol. Liq. 229 (2017) 217–220.
[58] L. Saiz, E. Guardia, J.A. Padro, J.Chem.Phys. 113 (2000) 2814–2822.